Geophysica (1994), 30, 1-2, 57-77

The Earth's Magnetic Field Maps of 1990.0

L. J. Pesonen[1], *H. Nevanlinna*[2], *M.A.H. Leino*[1] *and J. Rynö*[2]

[1]Geological Survey of Finland, Department of Geophysics, FIN- 02150 Espoo, Finland
[2]Finnish Meteorological Institute, Department of Geophysics, FIN-00100 Helsinki, Finland

(Received: August, 1994; Accepted: October, 1994)

Abstract

A series of maps of the Earth's magnetic field for the epoch 1990 are presented. The maps have been drawn on the basis of the spherical harmonic coefficients (SHCs) of the International Geomagnetic Reference Field (IGRF) of 1990.0 with the maximum degree and order of 10. The maps are shown as contour charts, where continents are outlined to help the geographic identification of specific features and anomalies. Besides the most common field elements, such as the declination (D), the inclination (I) and the total intensity (F), we also present maps describing the non-dipole field and the secular variation of the vertical component of the total field during the past decade (1990-1980). No significant changes (drift) in location of the major foci of the total or of the non-dipole field anomalies from those of the IGRF 1980-maps can be recognised. However, there are regions where the field has been rapidly changing during the past decade, for example in the Central Atlantic, where the vertical intensity has rapidly decreased and in the Indian Ocean, where it has increased.

A new way to analyse the Earth's magnetic field is to split its harmonic content into two families, the primary (dipole) and the secondary (quadrupole) field families, respectively. Contour maps of the vertical component of these field families for 1990.0 are presented. Moreover, a map depicting the vertical component of the "non-dipole" part of the dipole family field is included. The digitized grid values of the IGRF 1990 provided also an opportunity to study the departures of the present field from that of the Axial Geocentric Dipole Field (AGDF) and the dependence of some field parameters on geographic latitude. The former includes an analysis of inclination and total intensity, and the latter includes an analysis of the dispersion of directions and poles, the intensity of the non-dipole field and the secular change of the vertical component. These analyses reveal significant departures from the AGDF as well as pronounced hemispherical asymmetries in the present field. These departures and asymmetries are partly caused by the present tilt of the dipole axis and partly by the non-dipole field which is stronger and more variable in the southern hemisphere than in the northern one. The implications of these results on palaeomagnetic and palaeosecular variation studies are discussed.

1. Introduction

The Earth's magnetic field maps are used in many countries for practical and for scientific purposes like in navigation, in exploring the deep structures of the Earth, in geological mapping, in mineral exploration and even in biomagnetism to determine the orientation mechanism of some animals. In a co-operation between the Geological Survey of Finland (GSF) and the Finnish Meteorological Institute (FMI) global magnetic field charts have been prepared since 1983. The first series of these maps was based on the

IGRF of 1980.0 from the MAGSAT-mission (see e.g., *Langel et al.*, 1982; *Pesonen,* 1986) and were published in 1983 in national forums (*Nevanlinna et al.*, 1983; *Pesonen,* 1986; *Peltoniemi,* 1988). The maps showing the intensity of the total field and the non-dipole part of it have also been published in international textbooks (e.g., *Sharma,* 1986; *Fowler,* 1990).

One aim of this co-operation was to establish a tradition in map production so that new global magnetic maps will be made every ten years, which is just sufficiently long so that changes in the most rapidly varying field elements could be observed. With this in mind we begun in 1993 to prepare a new series of the Earth's magnetic field maps for the epoch 1990, after the spherical harmonic coefficients of the IGRF 1990.0 were released (*Langel,* 1992). Five maps of this series, the declination (D), the inclination (I), the total field intensity (F), the total intensity of the non-dipole field (F_{ND}) and the secular variation of the vertical intensity during the past decade ($DZ/Dt_{1990\text{-}1980}$) have already been published (*Pesonen et al.*, 1993). Here we present a complete series of ten maps describing the various features and anomalies of the IGRF 1990.0. After this, we analyse the departures of the present field from the AGDF and investigate the dependence of field elements on geographic latitude.

2. *The Earth's magnetic field*

The Earth's magnetic field can best be described with the help of the IGRF for a certain epoch. In deriving the reference field coefficients of 1990 we assume that the geomagnetic scalar potential V caused by internal magnetic sources, can be described in a form of spherical harmonic series (1):

$$V(r,\theta,\lambda) = R_e \sum_{n=1}^{N_{\max}} \left(\frac{R_e}{r}\right)^{n+1} \left[g_n^m \cos(m\lambda) + h_n^m \sin(m\lambda)\right] P_n^m(\cos\theta) \qquad (1)$$

where R_e is the radius of the Earth (6371.2 km), r is the distance from the center of the Earth, λ is the east longitude from Greenwich (°), θ is the geocentric colatitude (°), $P_n^m(\cos\theta)$ is the Schmidt-normalized Legendre's associate polynomial, with a degree of n and the order of m. g_n^m and h_n^m are the spherical harmonic coefficients determined from magnetic field measurements carried out all over the globe and which describe the relative strength of each harmonic term (n, m) in units of Tesla. In (1) n is the harmonic degree, the greatest value of which ($N_{\max}$) depends on the density of data of global measurements. Typically $N_{\max} = 8...13$, when the internal field originating from the liquid core of the Earth is analysed (*Nevanlinna*, 1986). Since the present analysis has been extended to $N_{\max} = 10$, the crustal anomaly contribution to the magnetic field components and maps is negligible.

The total component of the magnetic field intensity $\vec{F}$ is derived by taking the gradient of the potential (Eq. 2; *Nevanlinna et al.*, 1983):

$$\vec{F} = -\nabla V \tag{2}$$

The other elements like H (horizontal component), Z (vertical component), D (declination) and I (inclination) are defined as in (3):

$$H = \sqrt{X^2 + Y^2}$$

$$Z = \sqrt{F^2 + H^2}$$

$$D = arctan\left(\frac{Y}{X}\right) \tag{3}$$

$$I = arctan\left(\frac{Z}{H}\right)$$

where X and Y are the northern and eastern components of the H, respectively.

The following procedure was adopted in preparing the maps. We first calculated the values of each field element (say D) from the spherical harmonic coefficients of the IGRF 1990.0 (*Langel*, 1992) on the grid of 5° (latitude) x 5° (longitude) comprising the whole Earth. These values were drawn on Van der Grinten-world projections which include the continents to facilitate geographic identification of features in the maps and in naming the major anomalies. After this, contours were drawn using intervals of 10° for D, 5° for I and 2 to 4 μT for the intensity elements unless otherwise indicated. The interpolation and map drawing were partly done by computer and partly by hand.

3. *Description of the IGRF 1990-maps*

Declination and inclination

The two first maps (Figs. 1-2) shows the directional elements of the IGRF 1990: the declination (D_{1990}, Fig. 1) and the inclination (I_{1990}, Fig. 2). The zero declination line (Fig. 1) runs roughly in a N-S direction in Central European hemisphere, passes through northern Africa, turns to the east in southern Sudan, crosses the Indian Ocean and India and then turns to north-east over the Verkhoyansk mountain to the Arctic Sea. It reappears in northern Kamchatka, continues southwards in the eastern Pacific and Indonesia and ends up at the present South Magnetic Pole in the northern coast of Antarctica. In the other side of the world, the zero declination show up in the North American continent where it runs again in nearly N-S direction across the Americas. There are no significant changes in D from the 1980-declination map of *Nevanlinna et al.* (1983).

The most striking feature in the inclination map of Fig. 2 is the north-south hemispherical asymmetry: the northern hemisphere isolines of I are smoothly aligned in nearly E-W direction (showing dipolar dominance) whereas the southern hemisphere

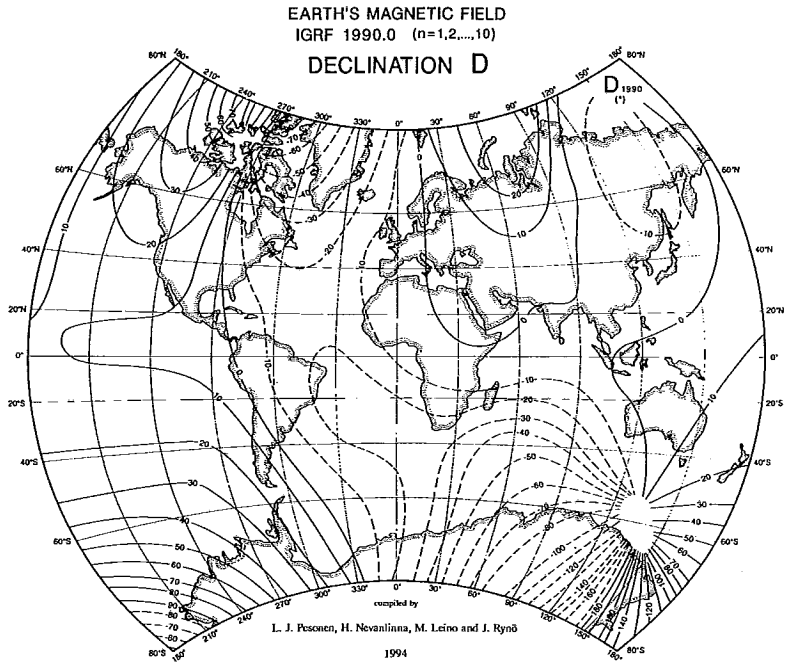

Fig. 1. Declination (D) of the IGRF 1990.0. Van der Grinten-projection of the world map. Contour interval is 10^{o}.

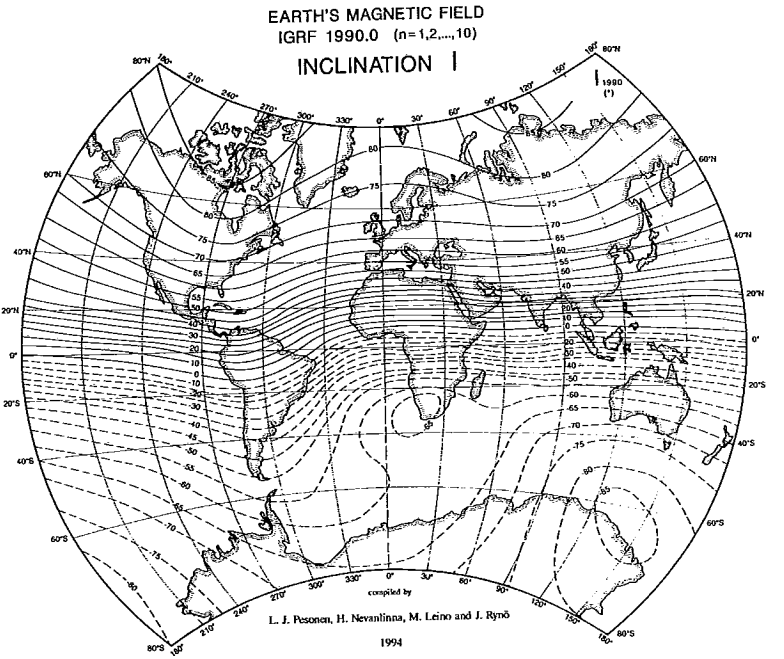

Fig. 2. Inclination (I) of the IGRF 1990.0. Contour interval is 5^{o}. Solid (dashed) lines denote positive (negative) inclinations.

isolines are more disturbed pointing to a pronounced non-dipole contribution. A few isolated inclination anomalies appear in the southern hemisphere, one in the SW corner of Africa (the -65°-anomaly) and one in NE Antarctica, close to S-magnetic pole (the -85°-anomaly). These anomalies show up at roughly the same locations as in the IGRF 1980 inclination chart of *Nevanlinna et al.* (1983) and in the IGRF 1965-inclination chart of *Garland* (1971).

Total field

Fig. 3 shows the total field intensity F for 1990 in 2 μT contour intervals. Although the map shows the typical "dipolar" characteristics of total intensity (i.e., F increases from equator towards the poles), it also shows four large regional total field anomalies caused by the non-dipole sources within the liquid core. The foci of these anomalies are located in Siberia, in Canada, in South America (on the east coast of Brasilia) and in the Indian Ocean, south of Australia. We return to these anomalies later in describing the non-dipole field maps. When compared with the 1980 total intensity map of *Nevanlinna et al.* (1983) neither the amplitudes nor the foci of these anomalies have significantly changed during the past decade.

Non-dipole field charts

The maps in Figs. 1-3 showed the three main elements of the 1990 geomagnetic field where the dipole terms ($n = 1, m = 0, 1$) of the spherical harmonic coefficients (SHC) are dominating. The residual field in which the dipole terms are subtracted from the total field is called the *non-dipole field (ND)* amounting to 10-20 % of the total field. The non-dipole field is important in many aspects of geomagnetism, in archaeomagnetism and in paleomagnetism. For example, the non-dipole field is known from historical records to change more rapidly than the dipole field as best manifested by the west-ward drift of some of the non-dipole field anomalies (e.g., *Bullard et al.*, 1950). The non-dipole field is causing departures of the regional archaeomagnetic intensity curves from that of the global mean (e.g., *Evans*, 1987; *Yang et al.*, 1993; *Pesonen et al.*, 1995). The ND-field plays a major role in geomagnetic polarity transitions (e.g., *Hoffman*, 1985; *Pesonen and Nevanlinna*, 1988) and is causing the so-called polarity asymmetries as observed in some palaeomagnetic results (e.g., Nevanlinna and *Pesonen*, 1983; *Schneider and Kent*, 1988). Therefore, the detailed monitoring of the evolution of the non-dipole field features in time and space is warranted. Here we present three maps (Figs. 4-6) describing the 1990 non-dipole field and its anomalies.

The total intensity of the non-dipole field can be expressed in two ways (see *Nevanlinna et al.*, 1983). First, a *scalar* magnitude of the non-dipole field (F_{ND}') can be obtained from Eq. 4, where the dipole coefficients $\left(g_1^0, g_1^1, h_1^1\right)$ of the spherical harmonics are omitted in the analysis. We get:

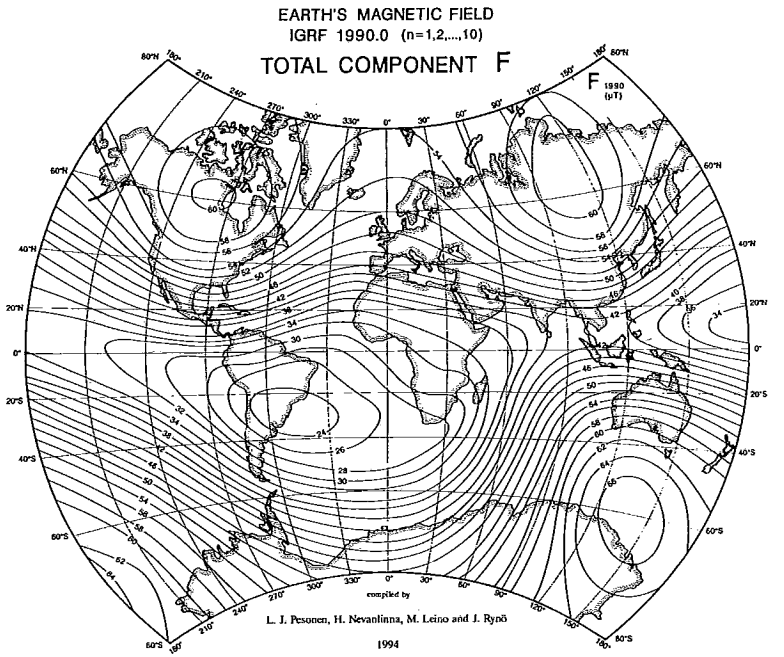

Fig. 3. Total component (intensity) (F) of the IGRF 1990.0. Contour interval is 2 μT.

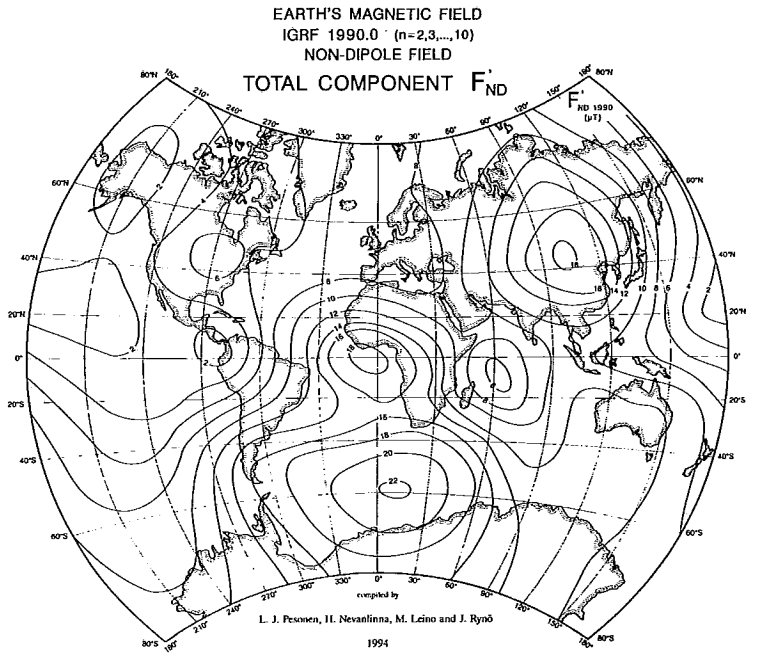

Fig. 4. Total component (intensity) of the non-dipole field (F_{ND}) of the IGRF 1990.0 as calculated from the Spherical Harmonic Analysis (SHA) with $n = 2,3,...,$ 10. Contour interval is 2 μT.

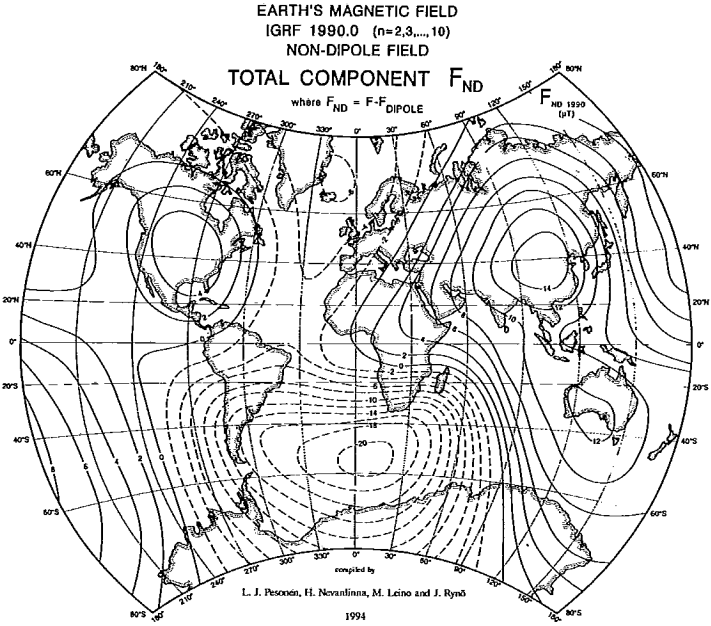

Fig. 5. Total component (intensity) of the non-dipole field (F_{ND}) of the IGRF 1990.0 as calculated from the equation $F_{ND} = F - F_{dipole}$ as explained in text. Contour interval is 2 μT. Solid (dashed) lines denote positive (negative) anomalies.

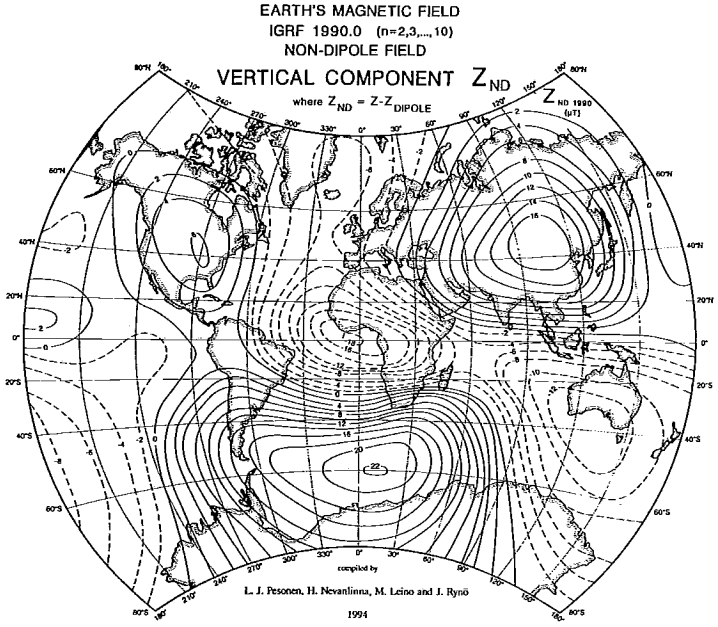

Fig. 6. Vertical component (intensity) of the non-dipole field (Z_{ND}) of the IGRF 1990.0. Contour interval is 2 μT. Solid (dashed) lines denote positive (negative) anomalies.

$$F_{ND}' = F\ (n = 2,..., 10) \tag{4}$$

where F_{ND}' denotes the total intensity of the non-dipole field being always positive, F is the total field and n is the degree.

The 1990 F_{ND}'-map is shown in 2 μT intervals in Fig. 4. Discarding the three minor anomalies with amplitudes of ≤ 2 μT, there are five regional total field non-dipole anomalies of which the largest one is in the South Atlantic Ocean and has an amplitude of 22 μT. This amounts up to 80 % of the total field in that area. It is this ND-anomaly which strongly contributes to the observed hemispherical asymmetries as seen in many maps of the IGRF 1990 (e.g., Figs. 5-7) and in many latitude dependent-curves of the field as will be shown in Chapter 4. Two of the *ND*-anomaly foci (the Siberian and the Canadian ones) are located slightly to the south of their corresponding total field foci of Fig. 3. One of the two remaining ND-anomalies is located in the central Atlantic, south of Ivory Coast and the other in the Seychelles Islands in the Indian Ocean (Fig. 4).

The other way to define the non-dipole total field intensity is to subtract arithmetically the dipole field (F_{dipole}) from the total field F at each grid point and by contouring the residual non-dipole field (5):

$$F_{ND} = F - F_{dipole} \tag{5}$$

where F_{ND} is the total intensity of the non-dipole field (μT).

Since the non-dipole field can locally enhance or reduce the dipole field, the F_{ND}-anomalies, as defined in (5), can either be positive or negative in sign. Therefore, this representation resembles a *vectorial* view of the non-dipole field intensity. Fig. 5 shows the F_{ND} contour map in 2 μT intervals. We can isolate four major non-dipole field anomalies of which three (the Siberian, the Canadian and the South Atlantic ones) are strikingly similar with those in the previous scalar map of the non-dipole field (Fig. 4). The two non-dipole anomalies on both sides of Africa of Fig. 4, however, disappear in the vector F_{ND}-map and some new anomalies show up, one in north of Iceland and one in south coast of Australia (Fig. 5). Note that the maximum F_{ND}-anomaly is again the South Atlantic one with an amplitude of -20 μT.

The most commonly used element to describe the non-dipole field is the intensity of the vertical component of the non-dipole field (Z_{ND}) (see e.g., *Stacey,* 1969, p. 130). Here it is defined as (6):

$$Z_{ND} = Z - Z_{dipole} \tag{6}$$

where Z is the vertical component of the total field vector and Z_{dipole} the vertical component of the dipole field, respectively.

Fig. 6 shows the Z_{ND}-map for 1990.0 in 2 μT intervals. We can isolate five major vertical component non-dipole field anomalies which all matches well with the total field

ND-anomalies in Figs. 4 and 5. Two of the Z_{ND}-anomalies (the Australian and the Ivory Coast ones) are negative while the three remaining ones (the Canadian, the Siberian and the South Atlantic ones) are positive. The locations and strengths of these *ND*-anomalies are strikingly similar with those of 1980.0 charts (*Nevanlinna et al.*, 1983) with no significant drift in location or change in amplitudes. However, investigation of slightly older Z_{ND}-maps reveal that some of these anomalies have been drifting. For example, if comparison is made with the 1945 Z_{ND}-map of *Stacey* (1969, p. 130) one can see that the Ivory Coast anomaly (with amplitude -18 μT) has been drifting ~10° *westwards* (corresponding to a drift rate of ~0.22°/yr) while the South Atlantic anomaly has been drifting ~25°*eastwards* (0.56°/yr).

Secular variation map

Although no significant changes in the anomaly foci of the total field can be identified during the past decade, it is possible that secular change in intensity has taken place. Secular variation of one of the field elements, namely the vertical intensity ($\Delta Z/\Delta t_{1990\text{-}1980}$), was calculated using Eq. (7):

$$(\Delta Z/\Delta t)_{1990\text{-}1980} = (Z_{1990} - Z_{1980})/10 \tag{7}$$

where ΔZ is the change in the intensity of Z between 1990 and 1980 (nT/year).

The overall view of $\Delta Z/\Delta t$-map (Fig. 7) shows the more pronounced secular change in Z in the southern hemisphere than in the northern one consistent with previous observations of hemispherical asymmetry of the IGRF 1990. A noticeable feature is the almost total lack of secular variation in the intensity of Z within Eurasia during the past decade. Three major secular variation anomalies in Z can be isolated in Fig. 7. The most intense $\Delta Z/\Delta t$-anomaly is located in central Atlantic with a maximum amplitude of -180 nT/year. The two other ones are both in the Indian Ocean, one just west of Australia (amplitude -40 nT/year) and the other to southeast from India (amplitude 80 nT/year). Although the morphology of the ΔZ map of 1990 has somewhat changed from the 1922.5- and 1942.5-maps (*Garland*, 1971, p.238) the above mentioned anomalies can be recognised also in these older maps.

Dipole and quadrupole families

A new insight into the geomagnetic field can be obtained by splitting the IGRF into two families, the primary (or, dipole) and the secondary (or, quadrupole) families, respectively (e.g., *McFadden et al.*, 1988). In spherical harmonic terms the dipole family contain all terms of g_n^m and h_n^m for which $n-m$ = odd. Correspondingly, the quadrupole family contains all terms for which $n-m$ = even.

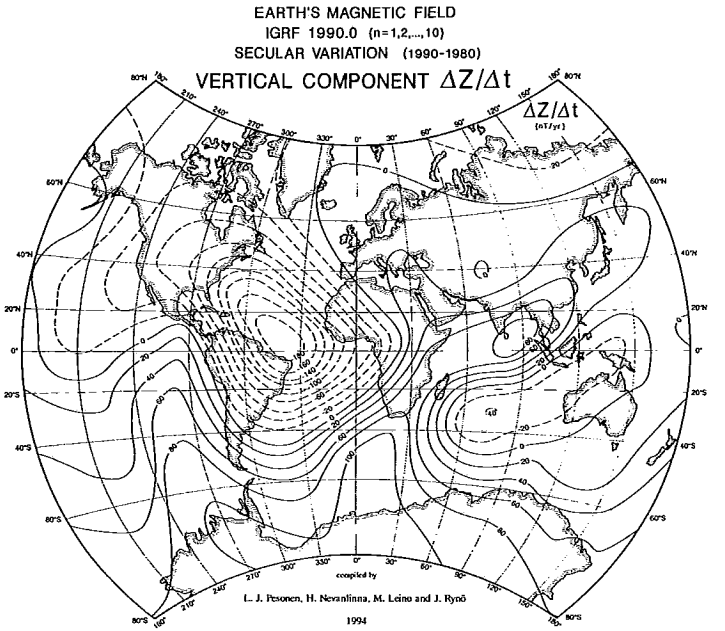

Fig. 7. Secular variation of the vertical component ($\Delta Z/\Delta t$) of the IGRF 1990.0 during the past decade 1990-1980. Contour interval is 20 nT/year. Solid (dashed) lines denote positive (negative) anomalies.

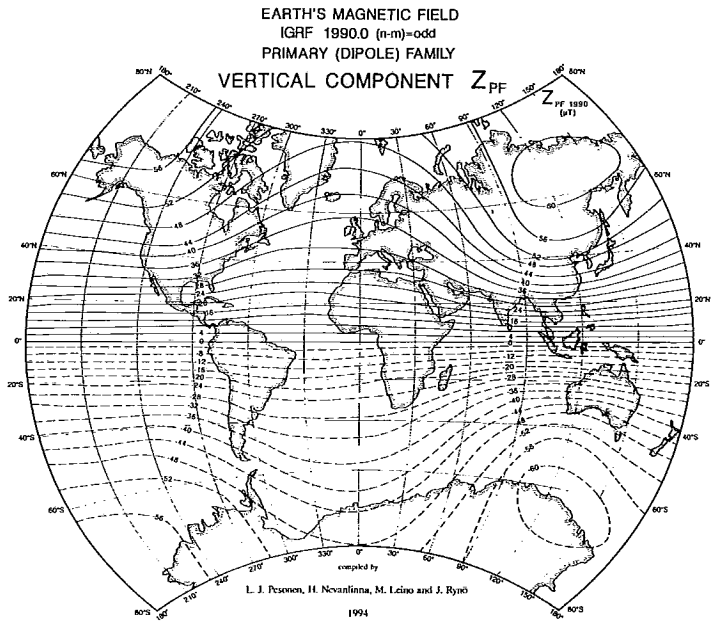

Fig. 8. Vertical component (Z_{PF}) of the primary (dipole) family field of the IGRF 1990.0. See text for explanation. Contour interval is 4 μT. Solid (dashed) lines denote positive (negative) anomalies.

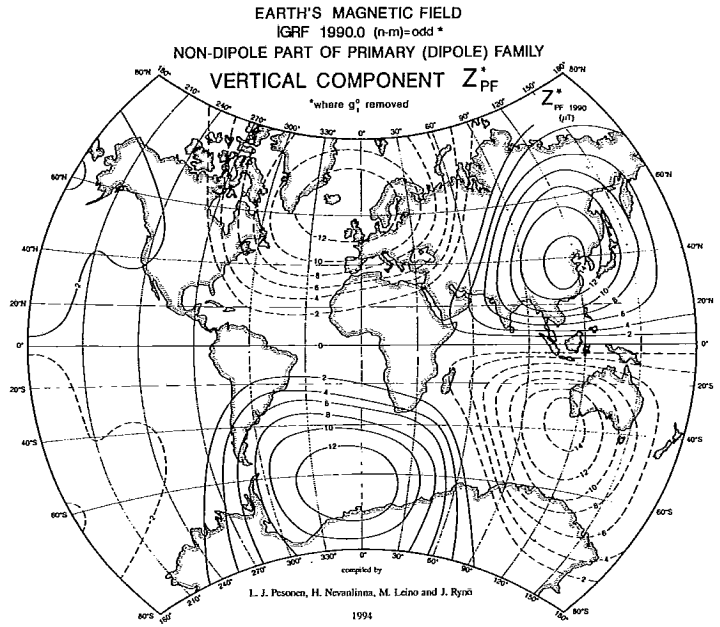

Fig. 9. Vertical component ($Z_{PF}{}^*$) of the "non-dipole" part of the primary (dipole) family field of the IGRF 1990.0 (i.e., term g^0_1 is removed from Z_{PF} of Fig. 8). See text for explanation. Contour interval 4 μT. Solid (dashed) lines denote positive (negative) anomalies.

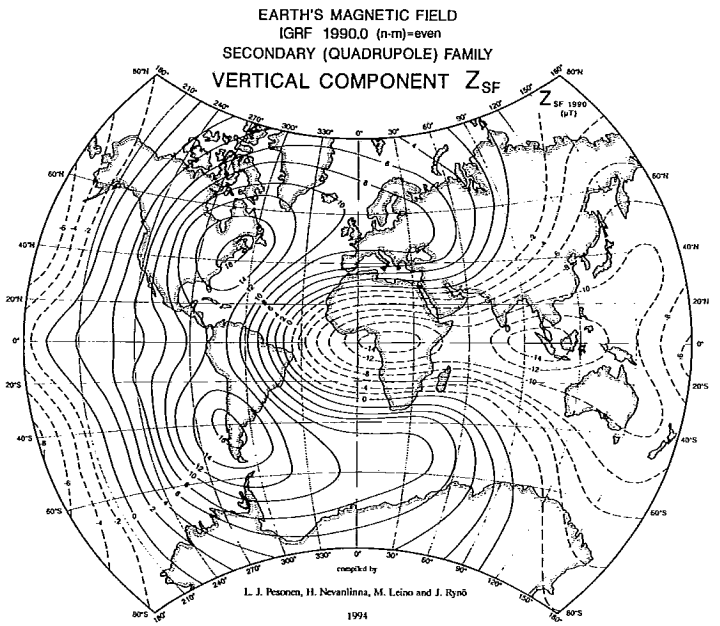

Fig. 10. Vertical component (Z_{SF}) of the secondary (quadrupole) family field of the IGRF 1990.0. See text for explanation. Contour interval 4 μT. Solid (dashed) lines denote positive (negative) anomalies.

Figs. 8-10 show the vertical component of the dipole and quadrupole families of the IGRF 1990.0, with 4 μT contour steps. We can observe that the dipole family map (Fig. 8) is featureless due to overwhelming dominance of the axial dipole term g_1^0. If we remove the axial dipole term g_1^0 from the dipole family map of Fig. 8, the remaining "non-dipole" map of the dipole family shows four distinct anomalies located symmetrically with respect to the equator (Fig. 9). The quadrupole family map (Fig. 10) shows also four distinct anomalies of which the two negative ones are located in Central Africa and in Malesia, and two positive ones are in the east coast of North America and in west coast of Chile, respectively.

4. *Present field and the AGDF*

One of the basic assumptions in paleomagnetism is that the long-term average of the geomagnetic field is that due to AGDF. If this assumption is fulfilled the inclination (I) of the field can be calculated directly from the geographic latitude (ϕ) by the well known dipole equation (8) (e.g. *Irving*, 1964, p. 43)

$$\tan I = 2 \tan\phi \tag{8}$$

We have studied whether the present (1990) field, which of course is only a snap-shot of the long-term field average, departs significantly from the AGDF.

Inclination

The mean inclination as a function of geographic latitude was calculated by averaging the inclinations of the IGRF 1990-grid data at 10° longitude intervals along latitude circles covering the whole Earth (from N to S pole) with a latitude step of 5°. Thus, 36 readings of inclination were obtained for each latitude circle (except at poles). Fig. 11 shows the result for 1990 inclination. The curves of I were calculated separately for the two hemispheres and their mean is also shown in Fig. 11. To allow a comparison, the inclination curve due to the AGDF is included (the dotted line). We can see that the overall shape of the 1990-inclination curves of the present field (N and S hemispheres) resemble those of the AGDF but the curves depart from each other, particularly at high latitudes. The mean curve matches the AGDF inclination curve at shallow to moderate latitudes (up to ~±60°) but departs from it at higher latitudes.These departures are partly due to the present tilt (~11.5°) of the dipole axis and partly due to non-dipole sources in the southern hemisphere. The departures would be less but do not disappear if geomagnetic latitudes had been used.

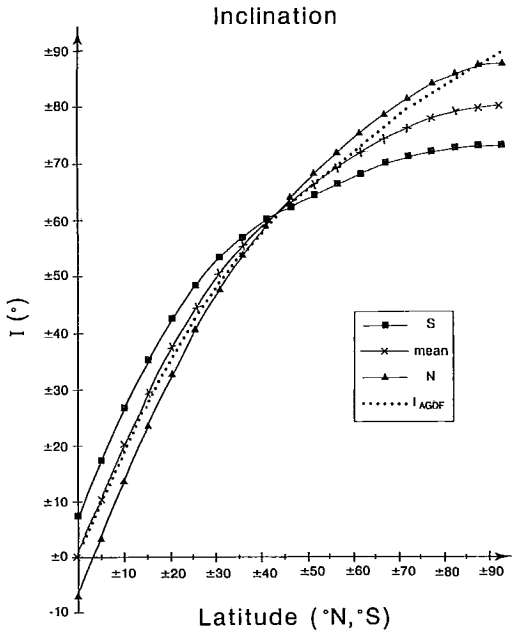

Fig. 11. Inclination I (degrees) of the IGRF 1990.0 plotted against the geographic latitude. S (N) denotes southern (northern) hemispheres, mean is their rms average, and I_{AGDF} is the inclination due to Axial Geocentric Dipole Field. See text for explanation.

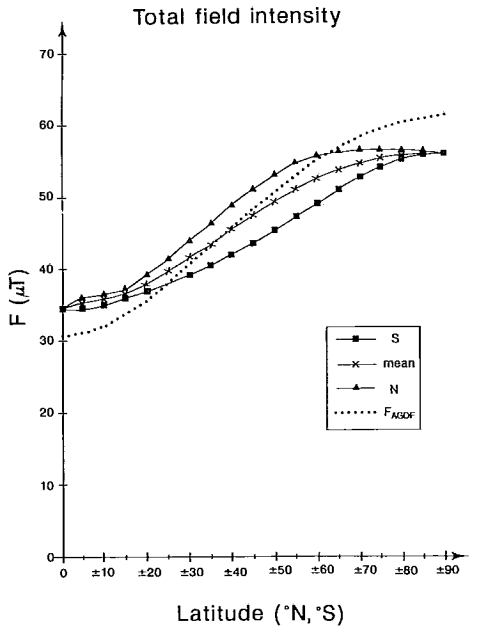

Fig. 12. Total field intensity F (μT) of the IGRF 1990.0 plotted against the geographic latitude. Other symbols as in Fig. 11.

Total intensity

In paleointensity studies, in order to make global comparison of measured intensities meaningful, the paleofield (F_p) must be transformed into an equatorial value F_e or into a Virtual Dipole Moment (*VDM*) to remove the major effect of latitude on intensity. The equatorial field intensity F_e can be calculated from the observed paleointensity F_p with the equation (9):

$$F_e = \frac{F_p}{\sqrt{4 - 3\cos^2\phi}} \tag{9}$$

where ϕ is the geographic (or palaeo-)latitude obtained from the inclination by Eq. (8) provided that the field is that due to the AGDF.

The intensity as a function of geographic latitude of the 1990-field was calculated using the same method as for inclination. We can notice in Fig. 12 that the shape of the intensity curves (N and S hemispheres, respectively) follow that due to AGDF-curve (dotted line) but depart from the latter at high latitudes. This is again mainly due to the present tilt of the dipole axis and partly due to non-dipole field. If geomagnetic latitudes were used instead of geographic ones the departures from the AGDF-curve would probably be much less. Notice also that the N and S curves depart from each other at middle latitudes due to the non-dipole field effects.

Dispersion of directions

One of the best known field elements which depends on latitude is the dispersion of field directions (e.g., *Creer*, 1962; *Irving and Ward*, 1964; *Halls and Pesonen*, 1982). The dispersion of directions can be expressed by scatter of directions (*D*, *I*) from their mean as calculated for each latitude. A measure for the scatter can be the circular standard deviation (Θ_{63}) (e.g., *Irving and Ward*, 1964) or the angular standard deviation (s) of field directions (*McFadden et al.*, 1988).

In this work we have calculated the dispersion of field directions (s) following the technique by *McFadden et al.* (1988). From the IGRF 1990 grid data we read the field directions (*D* and *I*) at 10° intervals of longitude along latitudinal circles covering the whole Earth from N to S geographic pole. The latitude step was 5°. The dispersion s of the field directions around their mean at a particular latitude ϕ is defined in Eq. (10):

$$s^2(\phi) = \frac{\sum_{i=1}^{N} \delta_i^2}{N-1} \tag{10}$$

where δ_i is the angle between the ith unit vector (defined by D and I) and the mean for that latitude, respectively, and N is the number of field directions. The mean of the field directions was calculated with Fisher statistics (*Fisher*, 1953) of the 36 unit vectors at each latitude circle. The dispersion s was calculated separately for the northern (s_N) and southern (s_S) hemispheres and the mean is the rms-value (see *McFadden et al.*, 1988).

The results are shown in Fig. 13. We can see that the dispersion of directions of the northern hemisphere decreases smoothly from equator to the pole, the decrease being more rapid at shallow latitudes. The dispersion in the southern hemisphere is very different. There is a weak decrease in s from ~10°S to ~40°S after which s slightly increases or levels off towards the pole. The rms-curve lies in between the northern and southern hemisphere curves with no well defined latitudinal dependence unlike in some other dispersion models (e.g., *Irving and Ward*, 1964). It is difficult to judge the significance of the observed hemispherical asymmetry in s since it is caused by both dipole and non-dipole variations of the field. The results may also depend on the way to analyse it as shown by *McFadden et al.* (1988). However, if the hemispherical asymmetry appears to be real, it may still be temporary so that the rms-curve in Fig. 13 is more representative of the long-term average of the directional dispersion as a function of latitude. If that is the case the rms-curve of Fig. 13 serves as a model for secular variation analysis (PSV) of ancient field directions (e.g., *Creer*, 1962).

Dispersions of Virtual Magnetic Poles (VGPs)

In PSV studies it has become more customary to plot the dispersion of VGP's versus latitude rather than the field directions, since the contribution of dipole wobble on dispersion will be eliminated when VGPs are used (e.g., *Cox*, 1970; *McFadden et al.*, 1988). The dispersion of VGP's of the IGRF 1990.0 was calculated using the same grid sampling technique as for field directions but VGP's now replacing the directions. In calculating the ith VGP from a D, I-pair, standard pole calculation routine was used (*Irving*, p. 1964, p. 43). Thus the mean VGP at a particular latitude is thought to be the one "viewed" by an observer at constant (Greenwich) longitude while the field is rotating a full circle. The longitude is arbitrary (since the field is rotating a full 360°) and Greenwich is chosen just for simplicity. The dispersion S of the VGP's at each latitude is now defined as the angular standard deviation by Eq. (11):

$$S^2(\phi) = \frac{\sum_{1=1}^{N} \Delta_i^2}{N-1} \tag{11}$$

where Δ_i is the angle between each VGP and their overall mean, and N is the number (=36) of VGP's for that latitude. The mean VGP was calculated using Fisher statistics. S was

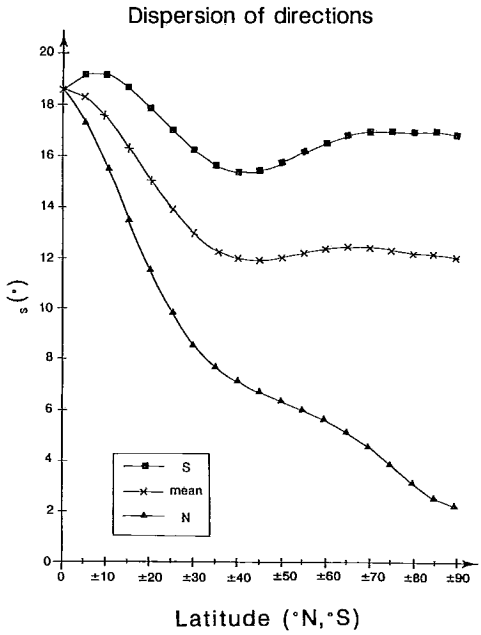

Fig. 13. Dispersion s of field directions plotted against the geographic latitude. s is the angular standard deviation of field directions (D,I) around their mean as explained in text. Other symbols as in Fig. 11.

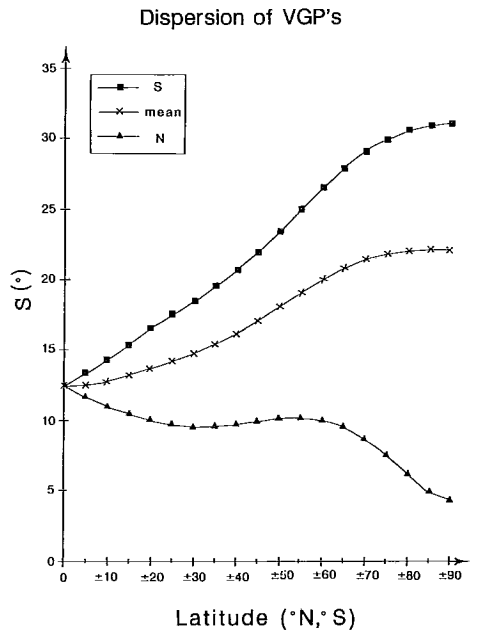

Fig. 14. Dispersion S of VGPs plotted against geographic latitude. S is the angular standard deviation of VGPs around their mean as explained in text (Eq. 11). Other symbols as in Fig. 11.

calculated separately for the northern (S_N) and southern (S_S) hemispheres to seek possible hemispherical differences; their global mean is the rms-value (*McFadden et al.*, 1988). The results are shown in Fig. 14.

The VGP-dispersion of the IGRF 1990 is virtually identical with that of the IGRF 1965 by *McFadden et al.* (1988).The southern hemisphere dispersion increases systematically from the equator to the pole while the northern one shows the opposite behaviour: the dispersion first decreases from equator to middle latitudes (~35°N) after which it remains stationary from 35°N to 60°N and finally decreases towards the N pole. The global dispersion increases from 12.5° at the equator to about 21.5° at poles. Since the VGP technique eliminates the contribution of dipole wobble on S, the likely explanation of the much larger value of S in the southern hemisphere is the more numerous and stronger non-dipole field sources in the southern hemisphere as seen in many previous maps (e.g., Figs. 4-6). We feel that the rms-curve of S in Fig. 14 best represents the long-term behaviour of the VGP-dispersion and should be used in secular variation studies of the ancient field.

Secular change in Z

The latitudinal dependence of the secular change Z-component during the past decade was investigated by calculating the mean (arithmetic) $\Delta Z/\Delta t$-values for each latitude as described previously. Fig. 15 shows the results. At shallow latitudes the secular change in Z is negative irrespective of the hemisphere. In the southern hemisphere the change in Z, however, increases from equator to the pole with changing sign at ~30°S, while it remains nearly stationary and negative throughout the northern hemisphere. The overall shape of the global mean curve of $\Delta Z/\Delta t$ follows that of the total intensity curve of Fig. 12 probably due to dipolar dominance in $\Delta Z/\Delta t$.

Non-dipole field

Fig. 16 shows the relative strength of the non-dipole field intensity as a function of latitude. The relative strength of the non-dipole field is here defined as the ratio of F_{ND}/F, where F_{ND} is the scalar non-dipole total field intensity (Eq. 4) and F is the total field intensity, respectively. The same method as previously was used to calculate its latitudinal dependence. The results are shown in Fig. 16. Again, we notice a clear hemispherical asymmetry, the non-dipole field being relatively much stronger on the average in the southern hemisphere than in the northern one. If we regard the global mean curve of Fig. 16 to represent the long-term average of the geomagnetic field, we can notice that the maximum non-dipole contribution is occurring at middle latitudes between 30°-60°. Although this can simply be a temporary feature of the 1990-field it may be a hint to understand the departures from the dipole field particularly observed at middle latitudes in the global analysis of the palaeomagnetic field (*Piper and Grant*, 1989).

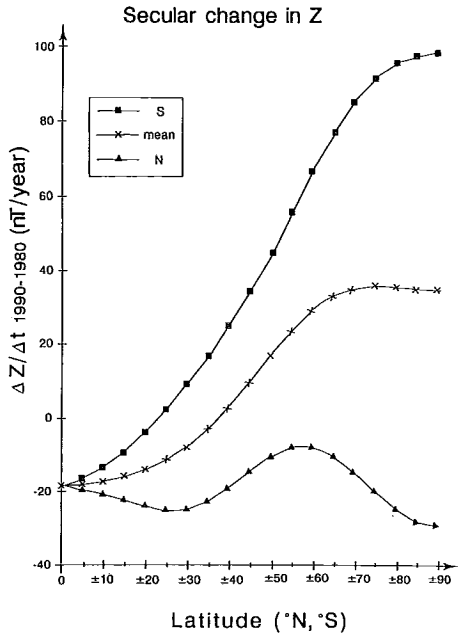

Fig. 15. Secular variation (nT/year) of the vertical component of IGRF 1990.0 (i.e. $\Delta Z/\Delta t$, where Δt = 1990-1980) plotted against the geographic latitude. See text for explanation. Other symbols as in Fig. 11.

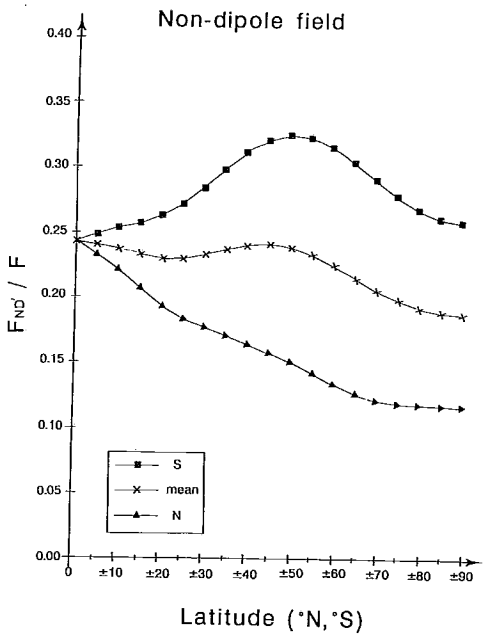

Fig. 16. The relative strength of the total intensity of the non-dipole field (F_{ND}/F) of the IGRF 1990.0 plotted against the geographic latitude. See text for explanation. Other symbols as in Fig. 11.

5. *Conclusions*

A series of maps has been prepared to describe the Earth's magnetic field at 1990. No significant changes in the foci of the field anomalies has occurred during the past decade but the field intensity is oscillating as seen in the analysis of secular change of the vertical component. The maps reveal striking hemispherical differences in many of the field elements of the IGRF 1990.0 (*Merrill et al.*, 1979). In particular the non-dipole field is not only much stronger but also shows a more pronounced secular variation in the southern hemisphere compared to northern hemisphere data. The 1990 inclination and total intensity curves depart from the AGDF-model curves partly due to present tilt of the dipole axis and partly due to non-dipole field. The mean dispersion of VGPs, when averaged over the globe, shows a steady increase from equator to pole in a similar fashion as found by *McFadden et al.* (1988) and serves as a tool to study secular variation of palaeomagnetic data.

Acknowledgements

Sisko Sulkanen, Marjo Kujala, Salme Nässling and Kirsti Blomster helped in drawing the maps. Harri Järvinen assisted in the analysis. We are grateful to all these people. Sincere thanks are due to Phil McFadden for describing the procedure of calculating the global VGP-dispersion.

References

Bullard, E.C., Freedman, C., Gellman, H. and Nixon, J., 1950: The westward drift of the Earths magnetic field. *Philos. Trans. R. Soc.* London, Ser. A, **243**, 67-92.

Cox, A., 1970: Latitude dependence of the angular dispersion of the geomagnetic field. *Geophys. J.R. astr. Soc.*, **20**, 253-269.

Creer, K.M., 1962. The dispersion of the geomagnetic field due to secular variation and its determination for remote times from palaeomagnetic data. J. Geophys. Res., **67**, 3461-3476.

Evans, M.E., 1987: New archaeomagnetic evidence for the persistence of the geomagnetic westward drift. *J. Geomag. Geoelectr.*, **39**, 769-772.

Fowler, C.M.R., 1990: The Solid Earth, An Introduction to Global Geophysics. *Cambridge University Press*, Cambridge, p. 33.

Fisher, R., 1953. Dispersion on a sphere. *Proc. R. Soc. London Ser.* A, 217, 295-305.

Garland, G., 1971: Introduction to Geophysics, Mantle, Core and Crust. W.B. Saunders Company, Toronto, 419 p.

Halls, H.C. and Pesonen, L.J., 1982: Palaeomagnetism in Keweenawan rocks. *In*: Wold, R.J., and W.J. Hinze (eds), Geology and Tectonics of the Lake Superior Basin. *Geology. Society of America, Memoir* **156**, 173-201.

Hoffman, K.A., 1985: Transitional behaviour of the geomagnetic field. *J. Geomag. Geoelectr.*, **37**, 139-146.

Irving, E., 1964: Paleomagnetism and Its Application to Geological and Geophysical Problems. *John Wiley & Sons*, New York, 399 p.

Irving, E. and Ward, M.A., 1964: A statistical model of the geomagnetic field. *Geofis. Pura Appl.*, **57**, 25-30.

Langel, R., Ousley, G., Berbert, J., Murphy, J., and Settle, M., 1982: The MAGSAT mission. *Geophys. Res. Lett.*, **9**, 243-245.

Langel, R.A., 1992: International Geomagnetic Reference Field: The Sixth Generation. *J. Geomag. Geoelectr.*, **44**: 679-707.

McFadden, P.L., Merrill, R.T., and McElhinny, M.W., 1988: Dipole/quadrupole family modelling of palaeosecular variation. *J. Geophys. Res.*, **93**, No. B10, 11583-11588.

Merrill, R.T., McElhinny, M.W., and Stevenson, D.J., 1979: Evidence for long-term asymmetries in the Earth's magnetig field and possible implications for dynamo theories.*Phys. Earth Planet. Inter.*, **20**, 75-82.

Nevanlinna, H., Pesonen, L.J. and Blomster, K., 1983: Earths magnetic field charts (IGRF 1980.0). Open File Report Q19/22.0/World/1983/1, Geophysics Department, Geological Survey of Finland, Espoo, Finland, 5 pp with maps in Appendices.

Nevanlinna, H., 1986: The Spherical Harmonic Analysis of The Earth's Magnetic Field and its Geophysical Interpretation. *In*: L.J. Pesonen (ed.), Magnetic maps and anomalies, A post-graduate course, TKK-V-GEO B 16, Helsinki University of Technology, Department of Mining, Economic Geology. Espoo, Finland, 48-76 (in Finnish).

Nevanlinna, H. and Pesonen, L.J., 1983: Late Precambrian Keweenawan asymmetric polarities as analyzed by axial offset dipole models, *J. Geophys.Res.*, **88**, 645-658.

Peltoniemi, M., 1988: Maa- ja kallioperän geofysikaaliset tutkimusmenetelmät. Otakustantamo, p. 74 (in Finnish).

Pesonen, L.J., 1986: Mapping the Earth's Magnetic Field with the MAGSAT-Satellite. *In*: L. J. Pesonen (ed.), Magnetic maps and anomalies, A post-graduate course, TKK-V-GEO 16, Helsinki University of Technology, Department of Mining, Economic Geology. Espoo, Finland, 27-47 (in Finnish).

Pesonen, L.J. and Nevanlinna, H., 1988: Two successive Reversal Transitions from Crete Described by a Two-Dipole Model with Standing and time Varying Components. *J. Geomag. Geoelectr.*, **40**, 77-94.

Pesonen, L.J., Nevanlinna, H., Leino, M.A.H., and Rynö, J., 1993: The Earth's magnetic field charts of 1990.0. *In*: S. Mertanen, A. Laiho and S. Tattari (eds.), XVI Geophysics Days and Remote Sensing Days. The Geophysical Society and The Society of Photogrammetry and Remote Sensing of Finland, Espoo, Otaniemi, 175-180.

Pesonen, L.J., Leino, M.A.H. and Nevanlinna, H., 1995: Archaeomagnetic Intensity in Finland During the Last 6500 years - Evidences for a Latitude Dependent Non-Dipole Field at ~500 AD. *J. Geomagn. Geoel.* (in press).

Piper, J.D.A. and Grant, S., 1989: A palaeomagnetic test of the axial dipole assumption and implications for continental distribution through geological time. *Phys. Earth Planet. Int.*, **55**, 37-55.

Schneider, D.A. and Kent, D.V., 1988: The paleomagnetic field from Equatoria Deep-Sea sediments: Axial symmetry and polarity asymmetry. *Science*, **242**, No. 4876, 252-256.

Sharma, P.V., 1986: Geophysical Methods in Geology. *Elsevier*, New York, pp. 168-169.

Stacey, F., 1969: Physics of The Earth. *John Wiley & Sons*, New York, p. 130.

Yang, S.J., Shaw, J. and Rolph, T., 1993: Tracking a non-dipole geomagnetic anomaly using new archaeointensity results from north-east China. *J. Geophys. Int.*, **115**, 1189-1196.